Asian Journal of Pharmaceutical Sciences 17 (2022) 219–229

Available online at www.sciencedirect.com

ScienceDirect

journal homepage: www.elsevier.com/locate/AJPS

Original Research Paper

Effect of the structure of ginsenosides on the *in vivo* fate of their liposomes

Chen Chen[a], *Jiaxuan Xia*[a], *Hongwei Ren*[a], *Anni Wang*[a], *Ying Zhu*[a,b], *Ru Zhang*[a], *Zicheng Gan*[a], *Jianxin Wang*[a,c,*]

[a] *Department of Pharmaceutics, School of Pharmacy, Fudan University & Key Laboratory of Smart Drug Delivery, Ministry of Education, Shanghai 201203, China*

[b] *Institute of Tropical Medicine, Guangzhou University of Chinese Medicine, Guangzhou 510006, China*

[c] *Institute of Integrated Chinese and Western Medicine, Fudan University, Shanghai 200040, China*

ARTICLE INFO

Article history:
Received 30 September 2021
Revised 21 November 2021
Accepted 13 December 2021
Available online 16 January 2022

Keywords:
Ginsenosides
Liposomes
Structure activity relationship
Rg3 liposomes
Long circulation
Tumor targeting
Glut 1

ABSTRACT

To utilize the multiple functions and give full play of ginsenosides, a variety of ginsenosides with different structures were prepared into liposomes and evaluated for their effect on the stability, pharmacokinetics and tumor targeting capability of liposomes. The results showed that the position and number of glycosyl groups of ginsenosides have significant effect on the *in vitro* and *in vivo* properties of their liposomes. The pharmacokinetics of ginsenosides liposomes indicated that the C-3 sugar group of ginsenosides is beneficial to their liposomes for longer circulation *in vivo*. The C-3 and C-6 glycosyls can enhance the uptake of their liposomes by 4T1 cells, and the glycosyls at C-3 position can enhance the tumor active targeting ability significantly, based on the specific binding capacity to Glut 1 expressed on the surface of 4T1 cells. According to the results in the study, ginsenoside Rg3 and ginsenoside Rh2 are potential for exploiting novel liposomes because of their cholesterol substitution, long blood circulation and tumor targeting capabilities. The results provide a theoretical basis for further development of ginsenoside based liposome delivery systems.

1. Introduction

For thousands of years, Panax ginseng C.A. Meyer has been widely used as a traditional precious medicinal material in China, Korea and Japan, and is known as the King of Herbs [1]. Ginsenosides have been proved as the main active ingredients of ginseng, and have been reported to be effective for various cancers. For instance, ginsenoside Rg3 and ginsenoside Rb2 treatment decreased both the number and size of tumor nodules in the liver, lung, and kidney tissues in a metastasis colorectal cancer (CRC) mouse model [2,3]. Ginsenoside Rg3 enhanced the anti-proliferative effects of erlotinib in BxPC-3 and AsPC-1 pancreatic cancer cells and xenograft [4]. Ginsenoside Rh4 significantly inhibited the growth of MCF-7 tumor cells *in vivo* [5]. Ginsenoside Rg3, Rh2 and Rg5 have a

* Corresponding author.
E-mail address: jxwang@fudan.edu.cn (J.X. Wang).
Peer review under responsibility of Shenyang Pharmaceutical University.

https://doi.org/10.1016/j.ajps.2021.12.002

significant synergistic anti-tumor effect with paclitaxel (PTX) in gastric cancer xenograft model [6]. According to the clinical data in China, ginsenoside Rg3 combined with chemotherapy could improve the survival rate of digestive system cancer patients and non-small cell lung cancer (NSCLC) [7,8]. However, ginsenosides have low bioavailability (BA) after oral administrationdue to the instability in gastrointestinal tract. They are easily degraded by intramuscular injection, which causes a short half-life and little tumor site distribution, and makes it difficult to effectively exert the curative effect [9,10]. Therefore, it is urgent to develop novel strategies to improve the pharmacological effect of ginsenosides.

Cholesterol has been proved having the ability to stabilize eukaryotic cell membrane phospholipids and widely applied as stabilizer in liposomal formulations [11]. However, excessive absorption of cholesterol into the blood may cause diseases such as hyperlipidemia, and studies have shown that cholesterol liposomes can cause allergic reactions [12]. The high cholesterol level in the tumor microenvironment is also related to the occurrence and development of tumors [13]. Researchers have carried out studies on cholesterol substitution in liposomes, and strived to find substitutes that can keep liposomes stable and have certain pharmacological effect, which include cholesterol derivatives, sterols and saponins with similar structures, such as β-sitosterol, ergosterol, lanosterol, ginsenosides and sea cucumber saponins [14–16]. In the previous studies in our lab, ginsenosides Rh2, Rg3, and Rg5 have been applied to replace cholesterol as stabilizer in liposomes, and have certain cancer cell targeting capabilities because of the high binding ability between the glycosyl group of ginsenosides and Glucose transporter 1(Glut 1) that highly expressed on the surface of tumor cells, and thus significantly inhibit the growth of gastric cancer, glioma and breast cancer [14,17,18]. These results proved that as a component of liposomes, some ginsenosides are not only an active ingredient, but also have the potential to replace cholesterol as membrane stabilizer and an active tumor targeting ligand.

Most of the ginsenosides belong to dammarane-type ginsenosides, which can be divided into protopanaxadiol (PPD) group and protopanaxatriol (PPT) group based on whether it has hydroxyl group at C-6 position. As illustrated in Fig. 1, PPD has glycosyl group attached to the β-OH at C-3 and/or C-20, while PPT has glycosyl group attached to the α-OH at C-6 and/or β-OH at C-20 [19]. It has been proved that the structure of ginsenosides have a great influence on their activities. The study on the structure-activity relationship of ginsenosides mainly focused on the number and position of glycosyl groups [20–22] and found that the cytotoxic effect of ginsenosides is negatively correlated with the number of glycosyl groups, and the order of their activities is monoglycoside > sapogenin > diglycoside > triglycoside > tetraglycoside [20,21]. The cytotoxicity of ginsenosides with different location of glycosides has been reported to be C-3 position > C-6 position > C-20 position [20,22].

However, the effect of ginsenosides with various structures, for example, with different position and number of sugar moieties attached to the dammarane-type ginsenoside, on the *in vivo* fate of their liposomes is still unclear. In this study, eight ginsenosides with different structure were selected based on the number of glycosyl on C-3, C-6 and C-20 position (Fig. 1A-1B) to systematically explore the relationship between the structure of ginsenosides and the characteristics of their liposomes, including stability, blood circulation time and tumor targeting effect. The results indicated ginsenosides have different influence on the stability of the liposomes after being incorporated into the phospholipid bilayer. C-3 sugar group of ginsenosides is not only beneficial to their liposomes for longer circulation in the blood, but ehance the cytotoxicity significantly. All tested ginsenosides have high affinity with Glut 1, and the uptake of liposomes by 4T1 tumor cells was mainly through the Glut transport pathway. The liposomes of ginsenosides with glycosyl at C-3 position, such as Rh2 and Rg3, have strong tumor cytotoxicity *in vitro* and tumor targeting effect *in vivo*. The study provides a basis for the research and development of novel liposomal system based on ginsenosides.

2. Materials and methods

2.1. Materials

Egg yolk lecithin (EPC) was purchased from AVT Pharmaceutical Co., Ltd. (Shanghai, China). mDSPE-PEG2000 was purchased from Ponsure Biotechnology (Shanghai, China). Cholesterol was purchased from Sinopharm Chemical Reagent Co., Ltd. (Shanghai, China). Ginsenoside Rh2 was purchased from Prefa Co., Ltd. (Shanghai, China). Ginsenoside Rh1, Rd, Rb1, Rf, Protopanaxdiol (PPD), Protopanaxatriol (PPT) were all purchased from Yuanye Co., Ltd. (Shanghai, China). Ginsenoside Rg3 was provided by Shanghai Ginpsome Pharmatech Co., Ltd. (Shanghai, China). DiR iodide (1,1‘-dioctadecyl-3,3,3’,3‘-tetramethylindotricarbocyanine iodide) and DiD iodide (1,1‘-dioctadecyl-3,3,3’,3‘-tetramethylindotricarbocyanine perchlorate) were obtained from Meilunbio Co., Ltd. (Dalian, China). Glut 1 siRNA and si-RNA mate were obtained from Shanghai Gene pharma Pharmaceutical Technology Co., Ltd (Shanghai, China). Pure water was obtained by Milli-Q Integral (Merck, Germany).

2.2. Preparation of ginsenoside liposomes

All the liposomes were prepared by thin-film hydration method. Conventional cholesterol-based liposomes (Chol-lipo) were prepared with a formulation of EPC and cholesterol (10:3 in mass ratio), meanwhile, pure phospholipid liposomes were prepared with EPC only, named EPC. For ginsenoside liposomes (GS-lipo), cholesterol was replaced by different ginsenosides. PEGylated liposomes (Chol-PEG-lipo) were prepared by adding mDSPE-PEG2000 in the formulation with a mass ratio of 1:10:3. Briefly, all lipid materials were dissolved in 1 ml mixed solvent (Chloroform: ethanol = 1:1, v/v), and evaporated with rotary evaporator to form a thin film. Then the thin film was subsequently hydrated with 1 ml 5% glucose solution at 48 °C for 30 min, the liposomal suspension was subjected to a probing sonication process in an ice bath for 2 min (2sec sonication followed by 2sec rest) at 300 W. DiD-loaded and DiR-loaded liposomes were prepared by the

A

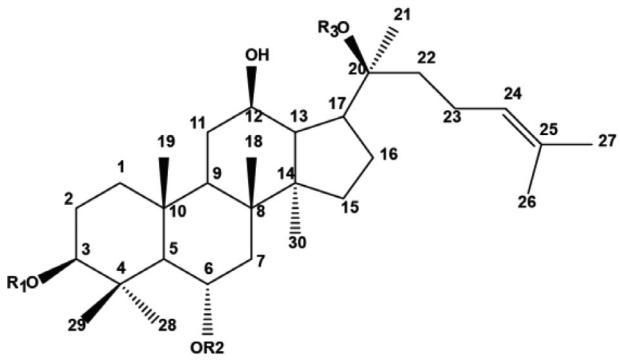

B

No.	Identification	C-3
1	protopanaxadiol(PPD)	-H
2	Rh2	-glc
3	Rg3	-glc(2-1)glc

No.	Identification	C-6
1	protopanaxatriol(PPT)	-H
2	Rh1	-glc
3	Rf	-glc(2-1)glc

No.	Identification	C-20
1	Rg3	-H
2	Rd	-glc
3	Rb1	-glc(6-1)glc

Fig. 1 – (A) The core structure of ginsenosides. (B) Ginsenoside structure with 0, 1, 2 glycosyl groups attached to position C-3, C-6 and C-20, respectively.

same method by adding the probe at the ratio of 2.5 to 1000 (DiD/lipid, w/w).

2.3. *Characterization of ginsenoside liposomes*

The particle size and ζ-potential of all liposomes were detected by a dynamic light scattering (DLS) detector (Zetasizer, Nano-ZS; Malvern, UK). All measurements of particle size and zeta potential were carried out after formulations were diluted in pure water with a volume ratio of 1/100. Transmission electron microscopy (TEM, Tecnai G2 F20 S-Twin, FEI, USA) was employed to collect the morphology, size, and structure of liposomes. For TEM, the liposomes were dripped onto copper grids and stained with uranyl acetate (2%, w/v).

2.4. *Stability of ginsenoside liposomes*

To evaluate the stability of ginsenoside liposomes, the size change of the liposomes stored at 4 °C were measured for 7 d. To investigate the stability improving mechanism of ginsenoside liposomes, the micropolarity of Chol-lipo, GS-lipo and pure phospholipid liposomes were measured and compared [23,24]. In brief, 20 mg pyrene were dissolved in acetone and diluted to a concentration of 4×10^{-7} mol/l. Then 0.5 ml pyrene solution was transferred to a test tube, placed in a fume hood to evaporate acetone. 0.5 ml liposomes was diluted for10 times and added to the tube, ultrasonicated for 10 min. Then the fluorescence intensity was detected after 12 h by setting the excitation wavelength at 338 nm. The absorbance values of the first and third absorption peaks were measured, respectively, and represented by I_1 and I_3.

2.5. *Pharmacokinetics of ginsenoside liposomes in mice*

The pharmacokinetics (PK) of various liposomes in normal male ICR mice (28-30 g) was studied [25]. Chol-lipo and Chol-PEG-lipo were chosen as controls, and 8 groups ginsenoside liposomes (GS-lipo) were administrated to the mice, respectively. DiD was chosen as fluorescence probe. 200 µl liposomes were injected into the mice tail vein, and blood samples were taken at 2 min, 5 min, 10 min, 20 min, 30 min, 1 h, 3 h, 6 h, 12 h, 24 h and 48 h from the mandibular vein after the injection. Blood samples were diluted 5 times with PBS to measure the fluorescence intensity (DiD excitation and emission wavelength were 644 nm and 680 nm, respectively). Then the percentages of residual fluorescence at each point to the initial fluorescence amount (the value at 2 min) were calculated to draw a fluorescence intensity percentage - time curve. DAS 2.0 pharmacokinetic software was used to calculate pharmacokinetic parameters, including half-life ($T_{1/2}$), area under the drug-time curve ($AUC_{0\rightarrow t}$) and mean residence time ($MRT_{0\rightarrow t}$), to compare the metabolic elimination of various liposomes.

2.6. *Cellular uptake of ginsenoside liposomes*

In order to compare the uptake capacity of triple-negative breast cancer cells (4T1) to different ginseng liposomes, 4T1 cells were seeded at a density of 2×10^5 cells per well, and DiD-labeled GS-lipo and Chol-lipo with a final DiD concentration of 500 ng/ml were added, respectively. The cells were incubated at 37 °C, 5% CO_2 for 4 h, and washed with pre-cooled PBS for three times to remove residual liposomes. Then the cells were digested and transferred to 1ml EP tube, washed twice with PBS, resuspended in 200 µl PBS, and determined the fluorescence intensity of each group by flow cytometry.

2.7. *Tumor targeting evaluation of ginsenoside liposomes*

To evaluate the tumor targeting capability of ginsenoside liposomes, female BALB/c mice weighing between 17-19 g were selected. After injecting 5×10^5 4T1 cells into the mammary fat pad, the mice were returned to normal feeding condition. When the tumor volume grew to about 100 mm^3, the mice were randomly divided into nine groups ($n = 3$). Then 200 µl DiR-labeled GS-lipo was injected to the mouse with the same fluorescence intensity through the tail vein, respectively.

At 2 h, 4 h, 8 h, 12 h and 24 h after the injection, *in vivo* animal imaging was applied to measure the change of fluorescence intensity. The fluorescence value of tumor site of each mouse was compared by calculating the fluorescence intensity of the region of interest (ROI). The mice were anesthetized at 24 h to dissect the tumor, heart, liver, spleen, lung and kidney to measure the fluorescence intensity. Graphpad prism 7.0 was used for statistical difference calculation.

2.8. Cytotoxicity of free ginsenosides and ginsenoside liposomes

The 3-(4,5)-dimethylthiahiazo(-z-yl)-3,5-diphenytetrazolium–romide (MTT) method was applied to investigate the cytotoxic effect of free ginsenosides and ginsenoside liposomes on 4T1 cells. 5×10^3 cells per well were seeded in a 96-well plate, placed in incubator overnight, and then added different ginsenosides or GS-lipo. Ginsenosides were dissolved in dimethyl sulfoxide (DMSO) except Rb1, which needs to be dissolved in methanol to prepare a concentrated solution. The plastids are gradually diluted with culture medium for 2 times as the lowest concentration. The maxium concentration of DMSO was lower than 1/200. After incubated for 48 h, 0.5 mg/ml MTT solution was added and incubated for 4 h at 37 °C, 5% CO_2, and then the MTT and medium mixture was carefully aspirated. After that, 150 μl of DMSO was added to dissolve formazan. The absorbance were then detected at 490 nm and 570 nm wavelengths to calculate the median inhibition concentration (IC_{50}) values of ginsenoside liposomes and free ginsenosides with Graphpad prism 7.0. The cell viability calculation formula is as follows:

$$\text{Cellviability}(\%) = \frac{OD_{sample} - OD_{medium}}{OD_{control\ group} - OD_{medium}} \times 100\% \quad (1)$$

2.9. Molecular docking of ginsenosides and Glut 1 transport

In order to elucidate the interaction between ginsenosides and Glut 1 transporter, which is highly expressed on the surface of many tumor cells, molecular docking was conducted. Firstly, the structural formulas of each ginsenosides and cholesterol were downloaded from Scifinder website. Secondly, the structures of cholestrol and ginsenosides were saved with ChemDraw 2D and the saved pictures were opened with ChemDraw 3D. Then minimum energy process was performed, and the resulting structure diagram was saved in PDB format. Thirdly, the Glucose transporter 1 (Glut 1) secondary structure was downloaded from Protein data bank, saved in PDB format, and opened with Maestro11.8. After pre-processed, ginsenosides and cholesterol molecules, were processed to generate their possible conformational structures respectively, and then each conformation was docked with Glut 1. Finally, the dock scores were calculated and obtained. The higher of the absolute score value, the stronger the hydrogen bond interaction between the molecule and the Glut 1, and the tighter of the binding between the ligands and Glut 1. Python was used for processing to mark the position of the interaction between ligands and Glut 1.

Table 1 – Characterization of ginsenoside liposomes ($n = 3$; mean ± SD)

Liposomes	Size (nm)	PDI	Zeta Potential (mV)
Chol-lipo	103.82±2.01	0.264±0.012	-27.9±1.03
PPD-lipo	82.62±1.15	0.251±0.082	-22.4±1.01
Rh2-lipo	111.92±1.21	0.173±0.021	-20.4±0.03
Rg3-lipo	93.06±1.51	0.132±0.011	-30.8±0.11
PPT-lipo	95.59±0.13	0.281±0.045	-37.9±0.12
Rh1-lipo	71.49±1.42	0.163±0.011	-23.2±0.08
Rf-lipo	86.62±1.10	0.242±0.012	-27.4±0.10
Rd-lipo	106.31±1.45	0.098±0.001	-29.5±1.20
Rb1-lipo	131.72±1.13	0.291±0.003	-25.2±1.03

2.10. Tumor cell uptake mechanisms of ginsenoside liposomes

To investigate the effect of Glut 1 on the cellular uptake of ginsenoside liposomes, the cell uptake after glucose receptor saturation and Glut 1 gene silencing was measured. 4T1 cells were cultured at a density of 2×10^5 cells per well. After the cells adhered to the wall, the medium was removed and PBS was added for starvation treatment for 15 min. Then 20 mM D-glucose solution was added and diluted in serum-free medium and incubate for 1 h. DiD loaded GS-lipo and Chol-lipo were diluted with medium and added to the cells for 4 h incubation respectively. The concentration of DiD in the system was 100 ng/ml. Then the medium was aspirated, the undigested DiD-labeled liposomes were washed away with pre-chilled PBS solution, to measure the fluorescence intensity with flow cytometer.

Glut 1 gene of 4T1 cell was knockout to verify its effect by Western blot and cell uptake. Glut 1 siRNA and siRNA mate were combined in opti-MEM medium, vortexed 10s, and stand for 15 min at room temperature to form siRNA complexes. Then siRNA complexe was added. After incubation for 72 h at 37 °C, 5% CO_2. The DiD-loaded GS-lipo and Chol-lipo were diluted with medium and added to the cells for incubation respectively. The concentration of DiD in the system was 100 ng/ml. The uptake amount of liposomes by 4T1 cells with and without Glut 1 gene knockout was detected and compared.

2.11. Statistical analysis

The values were presented as the mean ± standard deviation (SD) and analyzed using GraphPad Prism 7.0 software (GraphPad Software, CA, USA). Differences were assessed using one-way analysis of variance followed by the Newman-Keuls post-hoc test for multiple group comparisons and the t-test for comparisons between two groups.

3. Results and discussion

3.1. Characterization of liposomes

As shown in Table 1, the particle size of Chol-lipo and ginsenoside liposomes (GS-lipo) were 103.82 ± 2.01 nm and about 100 nm (82-132 nm), respectively. The PDIs of GS-lipo were less than 0.3, zeta potentials were around -25 mV, which

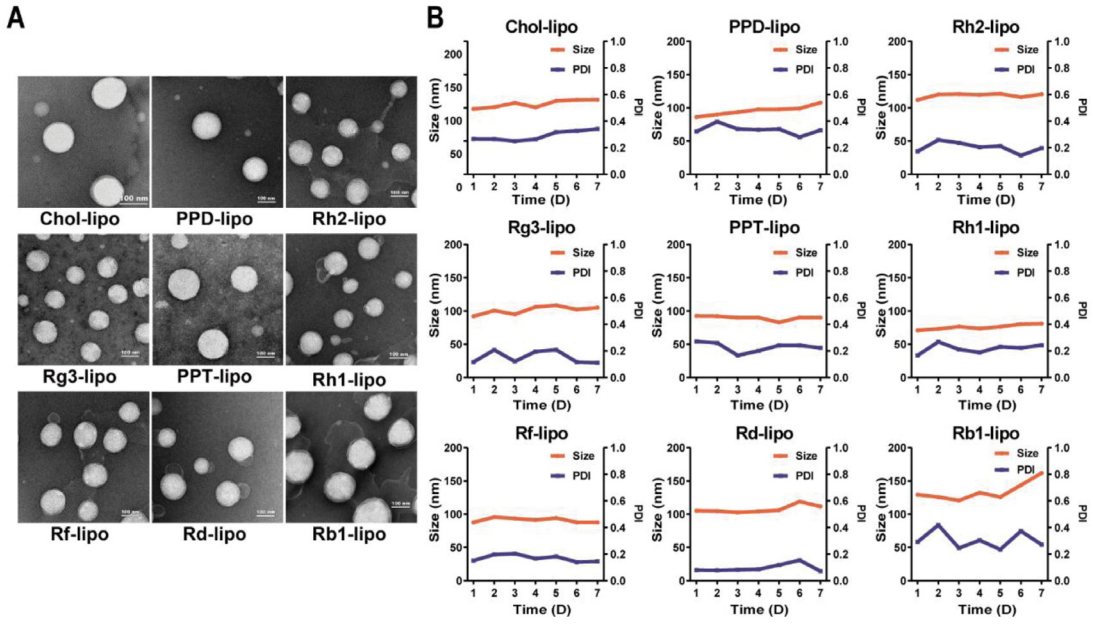

Fig. 2 – Characteristics of liposomes. (A) Morphology of cholesterol liposomes and various ginsenoside liposomes (scale bar = 100 nm). (B) Size and PDI changes of cholesterol liposomes and various ginsenoside liposomes at 4 °C for 7 d.

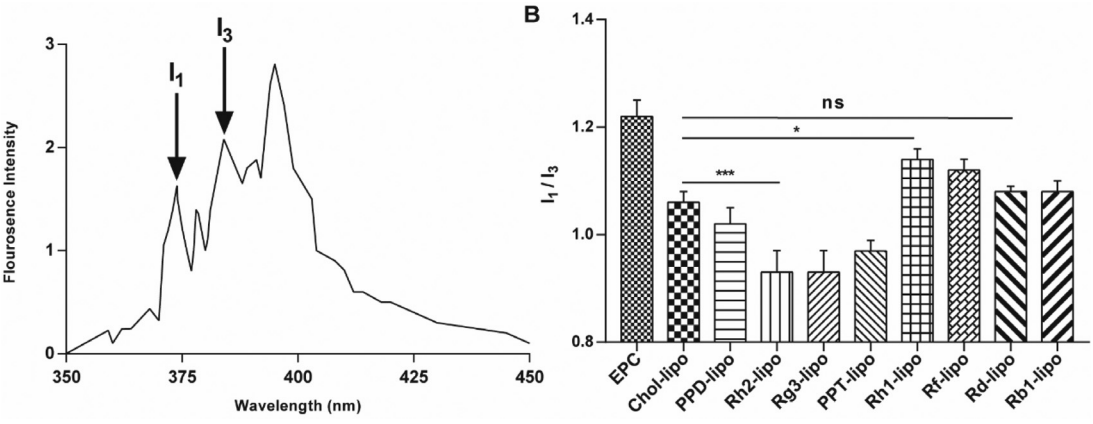

Fig. 3 – Micropolarity of liposomes. (A) The fluorspar spectra of pyrene. (B) Pyrene micro-polarity I_1/I_3 (378/383) in pure phospholipid liposomes (EPC), Chol-lipo and GS-lipos. ($n = 3$, mean ± SD). *$P < 0.05$, **$P < 0.01$,*$P < 0.001$.**

were similar to those of Chol-lipo. It could be seen from the morphology of liposomes (Fig. 2A) that both GS-lipo and Chol-lipo were relatively round and uniformly dispersed. The stability test results showed that all the liposomes were very stable with a narrow change of size and PDI at 4 °C for 7 d, except Rb1-lipo (Fig. 2B). For Rb1-lipo, the particle size increased from 129.2 ± 0.291 nm to 161.9 ± 0.271 nm during the storage. The possible reason for that is there are four glycosyl groups of ginsenoside Rb1, 2 attached at C-3 and 2 attached at C-20 position respectively, which may makes it hydrophilic and has a poor compatibility with the phospholipid bilayer. That may decrease the liposomes stability, thereby increasing the volume of Rb1-lipo.

The micropolarity of liposomes was measured to illustrate the stability mechanisms of ginsenosides. From the fluorescence scanning spectrum of pyrene (Fig. 3A), it could be found that there are five absorption peaks between 350-450 nm. The first absorption peak (373 nm) and the third absorption peak (384 nm), representing I_1/I_3, is related to the polarity of the environment and can reflect the arrangement of acyl groups in the environment where the pyrene probe located [23]. The smaller the I_1/I_3 value is, the lower the polarity between the lipid bilayers, indicating higher binding affinity between ginsenosides and phospholipid bilayers. The tight connection is beneficial to improve the physical stability and encapsulation efficiency of GS-lipos. The results showed that the micro-polarity of all the liposomes were less than pure phospholipid liposomes (EPC), demonstrating that both ginsenosides and cholesterol could interact with phospholipid molecules and enhance the stability of liposomes. The micro-polarity Rh2-lipo and Rg3-lipo with glycosyl groups at C-3 position were less than Chol-lipo, which meant that

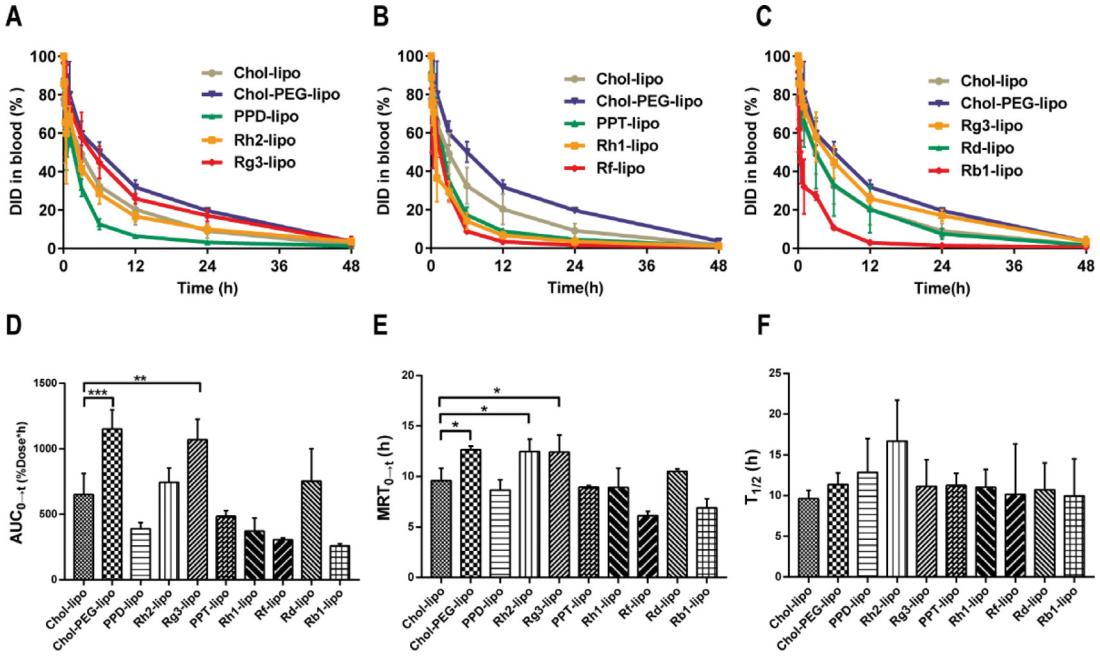

Fig. 4 – Pharmacokinetic profiles of various liposomes in ICR mice. The fluorescence intensity-time curves of ginsenoside liposomes with different numbers of glycosyl groups attached to positions C-3 (A), C-6 (B) and C-20 (C). (D-F) Pharmacokinetic parameters of ginsenoside liposomes with different glycosyl positions and quantities. ($n = 3$, mean ± SD). *P < 0.05, **P < 0.01, ***P < 0.001.

they had a stronger direct interaction with phospholipids and tightly inserted into the phospholipid bilayer. The membrane micropolarity of ginsenoside Rh1-lipo, Rf-lipo with glycosyl groups linking at C-6 position were higher than that of Chol-lipo, indicating that the sugars at positions C-6 may hinder the interaction between the ginsenosides and phospholipid, thereby they had a weaker binding ability with the phospholipid bilayer. The micropolarity of ginsenoside Rd-lipo and Rb1-lipo with glycosyl attached to C-20 were also significantly increased compared with Rg3 without glycosyl attached, but there was no significant difference compared with cholesterol, indicating that the liposomes at C-20 glycosyl had little effect on the interaction between ginsenosides and phospholipids (Fig. 3B).

3.2. *Pharmacokinetics of ginsenoside liposomes in mice*

The *in vivo* circulation time of ginsenoside liposomes was evaluated by measuring the relative residual amount of fluorescence intensity of DiD-labeled liposomes. The fluorescence intensity-time curve results proved that ginsenosides with glycosyl groups at C-3 position (Rg3 and Rh2) improve the *in vivo* circulation effects of GS-lipo (Fig. 4A), while ginsenosides with glycosyl groups at C-6 and C-20 descreased circulation time of the liposomes (Fig. 4B-4C). It also could be seen from the pharmacokinetic parameters that the $AUC_{0\rightarrow t}$ value of GS-lipo with two glycosyl groups attached to the C-3 position (Rg3-lipo) was significantly higher than that of Chol-lipo, and similar to Chol-PEG-lipo (Fig. 4D). The $MRT_{0\rightarrow t}$ values also indicated that the glycosyl linked to the C-3 position (Rh2-lipo and Rg3-lipo) improved the retention effect of GS-lipo *in vivo* (Fig. 4E). As for $T_{1/2}$, there is no significant differences among the various groups of GS-lipo (Fig. 4F). In summary, ginsenosides with the glycosyl attached to C-3 position of ginsenoside can improve the long circulation time of GS-lipo, and as the number increases, the long-term circulation effect is enhanced correspondingly.

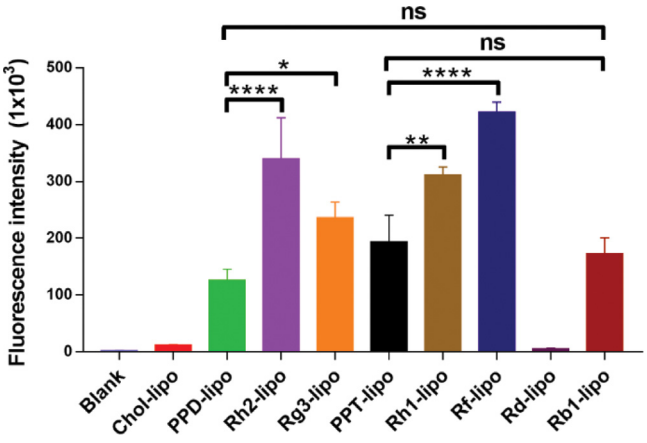

Fig. 5 – The uptake of ginsenoside liposomes with different glycosyl positions and numbers by 4T1 tumor cells. ($n = 3$, mean ± SD). *P < 0.05, **P < 0.01, ****P < 0.0001.

3.3. *Cellular uptake of ginsenoside liposomes*

As shown in Fig. 5, the uptake of ginsenoside liposomes by 4T1 cells was significantly higher than that of the Chol-lipo, except for Rd-lipo, demonstrating that ginsenosides were beneficial

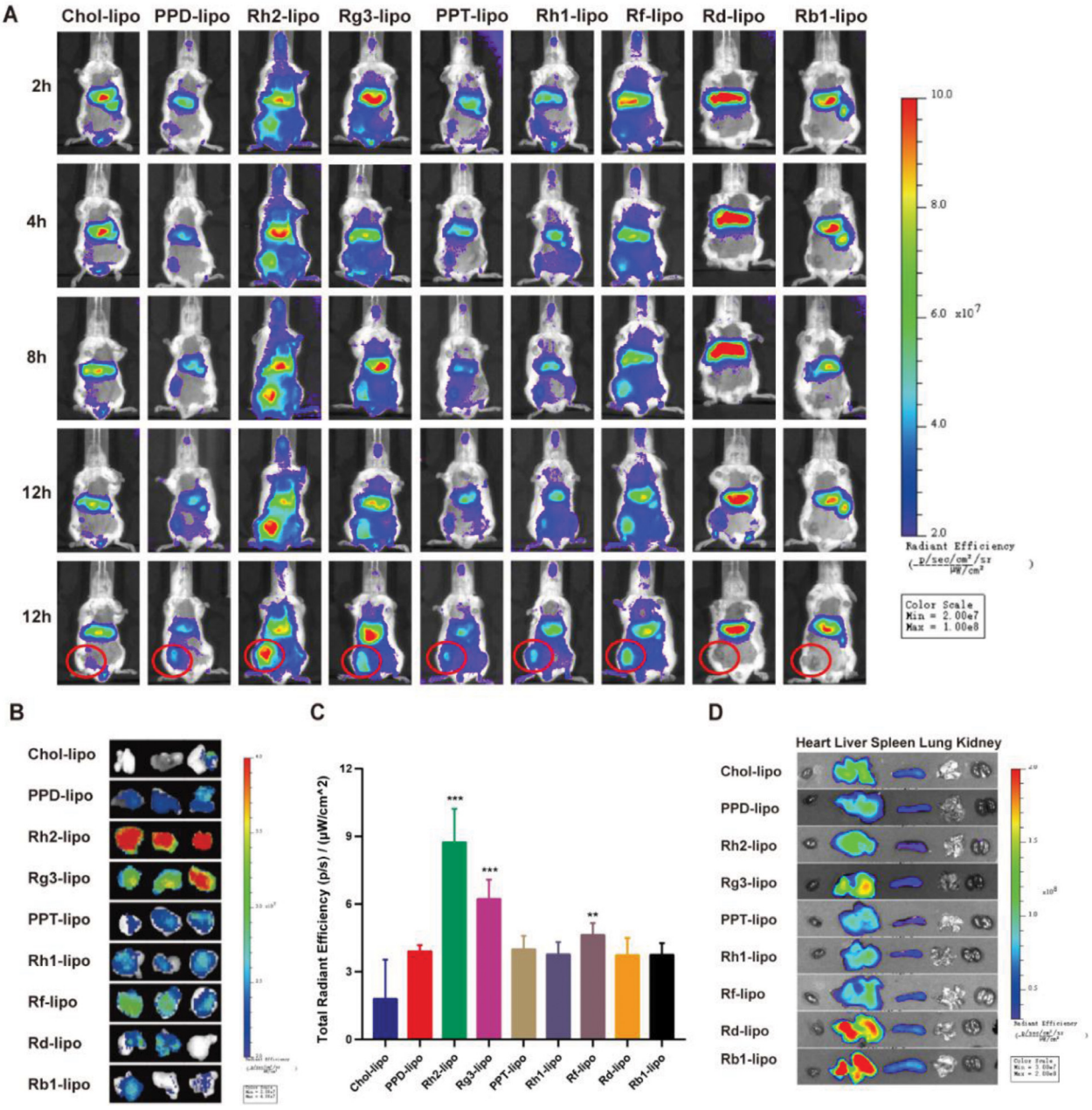

Fig. 6 – Tumor targeting of ginsenoside liposomes *in vivo*. (A) *In vivo* imaging of DiR-labeled in 4T1 tumor bearing mice. (B) *In vivo* imaging of tumors of Chol-lipo and GS-lipos. (C) Mean fluorescence intensity of tumor of Chol-lipo and GS-lipos. (D) Fluorescence images of biodistribution of Chol-lipo and GS-lipos in 4T1 tumor bearing mice 24 h. ($n = 3$; mean ± SD). **$P < 0.01$, ***$P < 0.001$.

to the tumor cell internalization of liposomes. The uptake of PPD-lipo and PPT-lipo, containing ginsenosides without glycosyl, significantly less than that of without glycosyl ginsenoside liposomes, Rh2-lipo and Rg3-lipo, Rh1-lipo and Rf-lipo. The results indicated that glycosyl may be involved in the incorporation. The cell uptake efficiency of GS-lipo with one and two glycosyl groups at C-3 and C-6 positions was significantly higher than those of GS-lipo with 1 and 2 glycosyl groups at C-20 position, indicating that the glycosyl ginsenoside liposomes connected at C-3 and C-6 positions are more conducive to the specific binding with the receptors on tumor cells and might attribute to tumor cell internalization of corresponding liposomes.

3.4. *Tumor targeting of ginsenoside liposomes*

Breast cancer orthotopic tumor model was established to investigate the *in vivo* tumor targeting effect of GS-lipo. DiR-labeled GS-lipos and Chol-lipo were administered through the tail vein respectively. From Fig. 6A, we found that the

fluorescence intensity of Rh2-lipo and Rg3-lipo groups were much stronger than that of Chol-lipo at all time points, indicating that Rh2, Rg3 and Rf could significantly promote the accumulation in tumor. In Rf-lipo group, in which Rf with two glycosyl groups attached to the C-6 position, had a weak active tumor targeting effect, while the GS-lipo with 0 and 1 glycosyl attached to the C-6 position, PPT-lipo and Rh1-lipo, basically had no targeting effect. These results indicated that ginsenosides with glycosyl groups attached to positions C-3 and C-6 had certain tumor targeting capabilities, while glycosyl groups attached to positions C-20 had no such effect, which coincided with the results of the tumor cell uptake experiment.

The mice were sacrificed after 24 h, and the tumors were taken out for imaging and fluorescence semi-quantitative analysis. As shown in Fig. 6B-6C, the fluorescence intensity of the tumor in Rh2-lipo, Rg3-lipo, and Rf-lipo groups were significantly stronger than that of Chol-lipo, which was consistent with the *in vivo* imaging results. The distribution amount in the liver and spleen of Rd-lipo and Rb1-lipo liposomes was higher than those of other groups, which might be caused by their specific recognition and phagocytosis of the macrophage system (MPS) during circulation in the body (Fig. 6D). Thus, ginsenoside liposomes with the glycosyl group attached to the C-20 not only have poor circulation effects according to the pharmacokinetic study, but also have poor tumor targeting ability.

All in all, both Rh2-lipo and Rg3-lipo showed significantly improved tumor targeting compared with Chol-lipo, since they could not only prolonged the systemic circulation but also enhanced the tumor cell uptake of the liposomes when they reached the tumor site. The results illustrated that the presence of the glycosyl group at C-3 position of ginsenoside plays an important role on the tumor targeting function of liposomes.

Based on the pharmacokinetics and tumor targeting results, it can be concluded that the position and number of glycosyls of ginsenosides significantly affect the *in vivo* fate of their liposomes. Among C-3, C-6 and C-20, the glycosyls at C-3 is important to the tumor distribution of ginsenoside liposomes. With the increase of glycosyl, the blood circulation time and tumor cell uptake of their liposomes were increased correspondingly.

3.5. *Cytotoxicity of free ginsenosides and ginsenoside liposomes*

Various free ginsenoside and GS-lipos with different concentration were given to 4T1 cells, respectively. From the IC_{50} of cytotoxicity result shown in Table 2, it was found that the ginsenosides with glycosyls (Rh2, Rg3, Rd, Rb1, Rh1, Rf) were less cytotoxic than those without glycosyl, PPD and PPT, which was consistent with previous reports [20,21].

When ginsenosides without glycosyl groups were prepared into liposomes, the cytotoxicity is significantly reduced. The IC_{50} of PPD and its liposomes were 16.29 ± 1.3 μg/ml and 87.9 ± 0.61 μg/ml; and the IC_{50} of PPT and its liposomes were 30.83 ± 1.05 μg/ml and 145.88 ± 3.26 μg/ml, respectively. The results indicated that the preparation of ginsenosides without glycosyl groups into liposomes hindered the cell entry and thus reduced their cytotoxicity.

Table 2 – IC_{50} of free ginsenosides and their liposomes.

Group		Ginsenoside	IC_{50} of free ginsenoside (μg/ml)	IC_{50} of ginsenoside liposomes (μg/ml)
Glucose number at C-3	0	PPD	16.29±1.3	87.9±0.61
	1	Rh2	33.08±1.04	21.97±0.7
	2	Rg3	154.52±11.2	117.21±8.01
Glucose number at C-6	0	PPT	30.83±1.05	145.88±3.26
	1	Rh1	-	-
	2	Rf	-	587.48±25.91
Glucose number at C-20	0	Rg3	154.52±11.2	117.21±8.01
	1	Rd	>300	338.84±5.42
	2	Rb1	-	390.84±1.25

However, when the glycosyl attached ginsenosides were prepared into liposomes, the cytotoxicity to 4T1 cells increased. For example, the IC_{50} of Rh2, with one glycosyl group at C-3 position, and its liposomes were 33.08 ± 1.04 μg/ml and 21.97 ± 0.70 μg/ml, respectively. The IC_{50} of Rg3 and its liposomes were 154.52 ± 11.2 μg/ml and 117.21 ± 8.01 μg/ml, respectively. When the concentration of Rb1 was 800 μg/ml, it had the effect on promoting cell growth with a cell survival rate of 120.13%. After being prepared into liposomes, its IC_{50} was 390.84 ± 1.25 μg/ml. The similar results were also found in Rh1 and Rf groups. Therefore, it could be conducted that after the glycoside-linked ginsenosides were prepared into liposomes, they were more conducive for ginsenosides to enter the cells and exert their cytotoxicity, indicating that the glycosyl groups play an important role in the cell uptake of liposomes. Rh2-lipo has the strongest cytotoxicity, followed by Rg3-lipo. It is speculated that glycosyl groups produced a certain specific recognition effect between the sugar groups and tumor cells, thereby increasing the cell entry rate and exerting stronger cytotoxicity.

3.6. *Molecular docking of ginsenosides and Glut 1*

Compared with the molecular docking score between cholesterol and Glut 1 (-6.42 ± 0.11), the scores of Rh2, Rg3, Rh1, Rf, Rd, Rb1 and Glut 1 were significantly lower, which were -7.55 ± 0.33, -8.374 ± 0, -7.45 ± 0.16, -9.150 ± 0, -8.43 ± 0.07, -10.46 ± 0.37, respectively (Fig. 7A), indicating they were closer to Glut 1 than cholesterol. There was no significant difference among the scores of PPD, PPT and cholestrol. The hydrogen bond interaction between ginsenosides and Glut 1 amino acid residue was analyzed, and the positions where the interaction happens were marked. Previous studies have shown that the amino acid residue positions of GLN161, GLN282, GLN283, ASN411 and TRP388 of Glut 1 are the key residues that glucose molecules bind with [26,27]. The results in Fig. 7B showed that the ginsenosides with glycosyls of more amino acid residues have stronger connecting ability with Glut 1 than cholesterol and ginsenosides without glycosyl, indicating that the glycosyl group is essential to enhance the interaction of ginsenoside liposomes with glucose transporter.

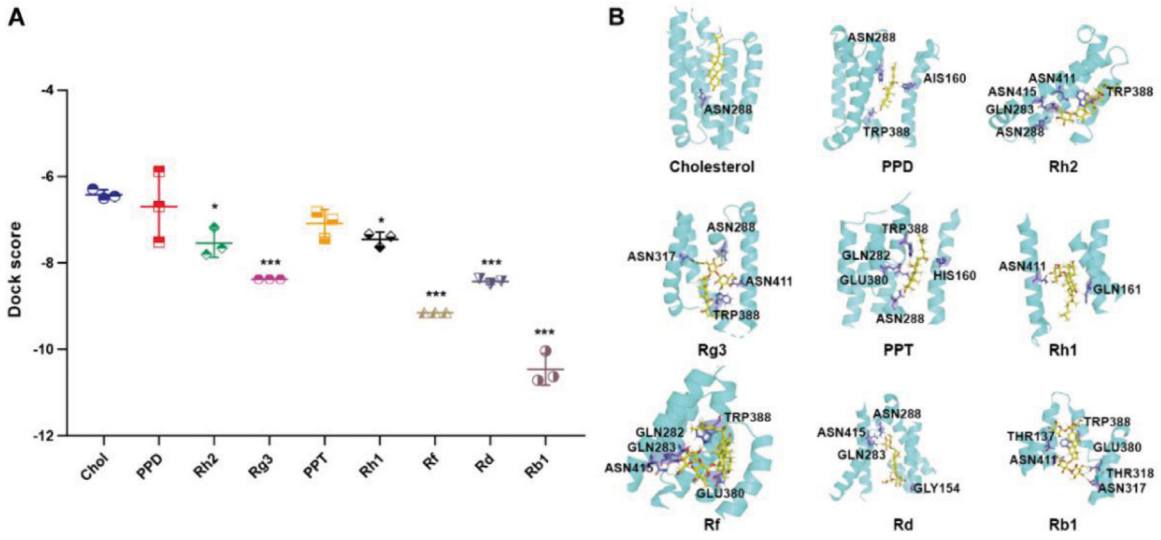

Fig. 7 – Molecular docking of ginsenosides with Glut 1. (A) Dock scores of cholesterol molecule and various ginsenosides docking with Glut 1. (B) 3D overlay interaction of Glut 1with cholesterol and ginsenosides. ($n = 3$, mean ± SD). *P < 0.05, ***P < 0.001.

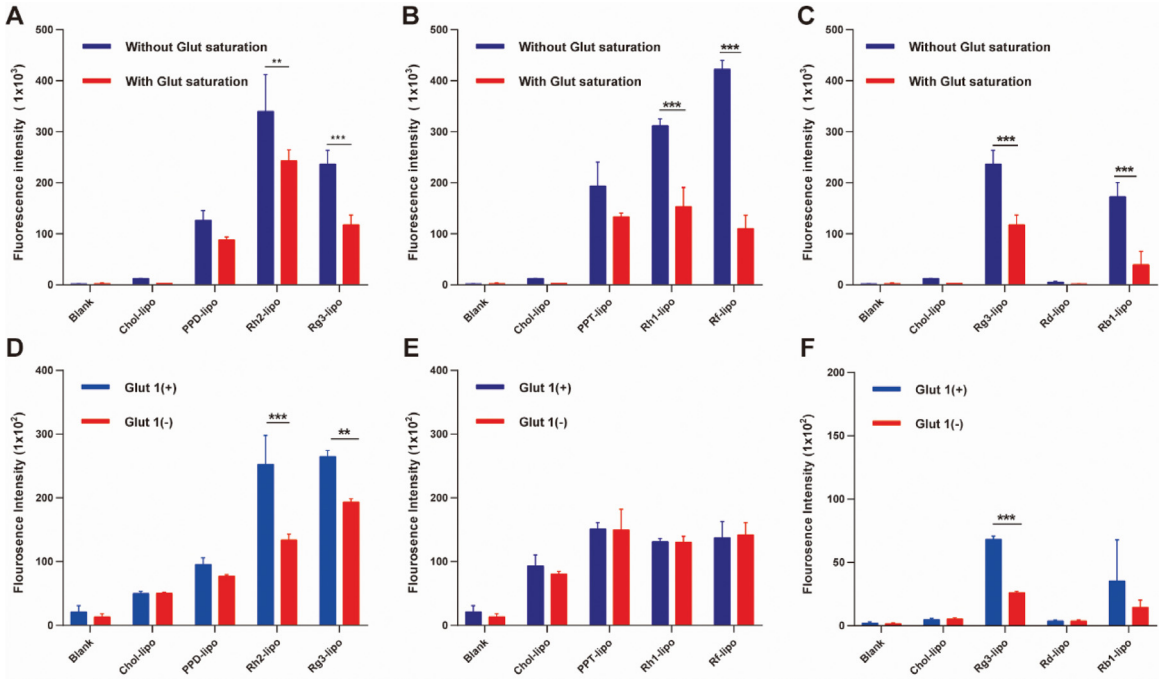

Fig. 8 – (A-C) The cellular uptake of ginsenoside liposomes with different number of glycosyl groups at C-3, C-6, C-20 positions by pre-saturated glucose receptor of 4T1 tumor cells ($n = 3$; mean ± SD), **P <0.01 and ***P <0.001. (D-F) The cellular uptake of ginsenoside liposomes with different number of glycosyl groups at C-3, C-6, C-20 ginsenoside liposomes before and after Glut 1 silencing. ($n = 3$; mean ± SD), **P <0.01 and ***P <0.001.

3.7. *Cellular uptake of ginsenoside liposomes after Glut saturated*

The rapid growth of tumor cells makes them require a large amount of glucose energy supply. However, since glucose molecule is polar hydrophilic, it cannot penetrate the hydrophobic cell membrane, and needs the help of a special type of transmembrane transporter-glucose transporter (Glucose Transporters, Gluts) [28], which were significantly up-regulated on the surface of tumor cells [29–31]. The massive consumption of glucose by tumors will inevitably increase glucose intake and Gluts involved in the process of glucose transport. In order to study the tumor cell targeting mechanism of ginsenoside liposomes, D-glucose solution

was added to pre-saturate the Gluts on 4T1 cells before the addition of liposomes for cell uptake. As shown in Fig. 8A-8C, the uptake amount of Rh2-lipo, Rg3-lipo, Rh1-lipo, Rf-lipo and Rb1-lipo significantly reduced after the pre-saturation of Gluts. In contrast, the uptake of Chol-lipo, PPD-lipo and PPT-lipo groups did not change significantly. The results indicated that the Gluts expressed on the surface of tumor cells play an important role in the cellular uptake of glycosyl-linked ginsenoside liposomes.

3.8. *Cellular uptake after Glut 1 silencing*

Glut 1 expresses on the cell membrane and participates in the transport of glucose to maintain the energy supply in the cell. Studies have shown that this protein is highly expressed on a variety of cancer cells, including 4T1 [32,33]. Previous studies in our lab showed that Rg3 can insert into the phospholipid bilayer of liposomes and one of the two glycosyl groups at C-3 exposes outside of phospholipid bilayer to bind with Glut 1 on the surface of cells, thereby exerting active targeting ability [17]. The uptake efficiency of various ginsenoside liposomes were compared before and after Glut 1 gene silencing by incubating with Glut 1 siRNA complexes.

As Fig. 8D-8F showed, the uptake of Rh2-lipo and Rg3-lipo in 4T1 cells was significantly reduced after Glut 1 gene silencing, while no change of uptake was found in other groups. The reason for this result is probably because this experiment only silenced one of the receptors that can transport glucose, i.e., Glut 1, and the glycosyl-linked ginsenoside liposomes still could be intaken by tumor cells through other transport pathways. The result also showed that Glut 1 expressed on the surface of 4T1 tumor cells does play an essential role in the cellular uptake of Rg3-lipo and Rh2-lipo groups. Since Glut 1 is the main transporter of glucose transporters, the strong binding of Rg3-lipo and Rh2-lipo with Glut 1 can effectively improve their tumor targeting ability.

4. Conclusion

Ginsenosides have a variety of pharmacological activities based on their specific chemical structure. In order to systematically investigate the relationship of liposome functionality and ginsenosides structure, eight ginsenosides with 0, 1, and 2 glycosyl groups attached to C-3, C-6, and C-20 position, respectively, were prepared into liposomes. It was found that the ginsenosides have different influence on the stability of the liposomes after being incorporated into the phospholipid bilayer. The micropolarity results showed that the glycosyl group at position C-3 facilitated the connection between ginsenoside and phospholipid, therefore increased the stability of the saponin liposomes. *In vivo* pharmacokinetics showed that the C-3 sugar group of ginsenosides is beneficial to their liposomes for longer circulation in the blood, while there is no such function of C-6 and C-20 glycosyls of ginsenoside for their liposomes. The results of cell uptake and cytotoxicity experiments proved that the glycosyl groups attached to C-3 and C-6 enhanced uptake effiency by 4T1 cells, and GS-lipo with glycosyl at C-3 had the strongest cytotoxicity. Based on molecular docking and Glut saturation experiment results, it was found that all tested ginsenosides had high affinity with Glut 1, and the uptake of GS-lipo with glycosyl groups at positions C-3, C-6 and C-20 by 4T1 tumor cells mainly through the Glut transport pathway. Tumor targeting and Glut 1 silencing results demonstrated that glycosyl at C-3 position enhanced the tumor active targeting ability significantly, based on the specific binding capacity to Glut 1 expressed on the surface of 4T1 cells. The study suggested that ginsenoside Rg3 and ginsenoside Rh2 are potential for developing novel liposomes with cholesterol substitution, long blood circulation and tumor targeting, and provided a theoretical basis for further clinical translation of ginsenoside liposomal delivery system.

Conflicts of interest

The authors declar no conflicts of interest.

Acknowledgment

This work was supported by the National Natural Science Foundation of China (No. 82074277 and 81773911), and the Development Project of Shanghai Peak Disciplines-Integrated Medicine (No. 20180101).

REFERENCES

[1] Park HJ, Kim DH, Park SJ, Kim JM, Ryu JH. Ginseng in traditional herbal prescriptions. J Ginseng Res 2012;36(3):225–41.
[2] Lan Thi Hanh P, Wijaya YT, Sari IN, Yang YG, Lee YK, Kwon HY. The anti-metastatic effect of ginsenoside Rb2 in colorectal cancer in an EGFR/SOX2-dependent manner. Cancer Med 2018;7(11):5621–31.
[3] Lan Thi Hanh P, Wijaya YT, Sari IN, Kim KS, Yang YG, Lee MW, et al. 20(R)-Ginsenoside Rg3 influences cancer stem cell properties and the epithelial-mesenchymal transition in colorectal cancer via the SNAIL signaling axis. Oncotargets Therapy 2019;12:10885–95.
[4] Jiang J, Yuan Z, Sun Y, Bu Y, Li W, Fei Z. Ginsenoside Rg3 enhances the anti- proliferative activity of erlotinib in pancreatic cancer cell lines by downregulation of EGFR/PI3K/Akt signaling pathway. Biomed Pharmacother 2017;96:619–25.
[5] Duan Z, Wei B, Deng J, Mi Y, Dong Y, Zhu C, et al. The anti-tumor effect of ginsenoside Rh4 in MCF-7 breast cancer cells *in vitro* and *in vivo*. Biochem Biophys Res Commun 2018;499(3):482–7.
[6] Hong C, Wang D, Liang J, Guo Y, Zhu Y, Xia J, et al. Novel ginsenoside-based multifunctional liposomal delivery system for combination therapy of gastric cancer. Theranostics 2019;9(15):4437–49.
[7] Guo XW, Hu ND, Sun G Z, Li M, Zhang PT. Shenyi Capsule plus Chemotherapy versus chemotherapy for non-small cell lung cancer: A systematic review of overlapping meta-analyses. Chin J Integr Med 2018;24(3):227–31.
[8] Pan L, Zhang T, Sun H, Liu G. Ginsenoside Rg3 (Shenyi Capsule) combined with chemotherapy for digestive system

cancer in China: A meta-analysis and systematic review. Evid Based Complement Alternat Med 2019 2019.
[9] Li J, Yl Dai, Zheng F, Xu CC, Feng L, Wang XY, et al. Oral absorption and *in vivo* biotransformation of ginsenosides. Chinese J Biologicals 2014;27(12):1633–6.
[10] Liiu JH, Lu D, Liu JP, Li PY. Studies on pharmacokinetics of 20(S)-Ginsenoside Rg3 after intramuscular administration to rats. Chinese Pharmaceutical J 2007;42(14):1087–90.
[11] Briuglia ML, Rotella C, McFarlane A, Lamprou DA. Influence of cholesterol on liposome stability and on *in vitro* drug release. Drug Delivery Translational Research 2015;5(3):231–42.
[12] Szebeni J, Baranyi L, Savay S, Bodo M, Morse DS, Basta M, et al. Liposome-induced pulmonary hypertension: properties and mechanism of a complement-mediated pseudoallergic reaction. American J Physiology-Heart Circulatory Physiology 2000;279(3):H1319–H1H28.
[13] Nelson ER, Chang CY, McDonnell DP. Cholesterol and breast cancer pathophysiology. Trends Endocrinol Metab 2014;25(12):649–55.
[14] Hong C, Wang D, Liang JM, Guo YZ, Zhu Y, Xia JX, et al. Novel ginsenoside-based multifunctional liposomal delivery system for combination therapy of gastric cancer. Theranostics 2019;9(15):4437–49.
[15] Muramatsu K, Maitani Y, Machida Y, Nagai T. Effect of soybean-derived sterol and its glucoside mixtures on the stability of dipalmitoylphosphatidylcholine and dipalmitoylphosphatidylcholine/cholesterol liposomes. Int J Pharm 1994;107(1):1–8.
[16] Li R, Zhang LY, Li ZJ, Xue CH, Dong P, Huang QR, et al. Characterization and absorption kinetics of a novel multifunctional nanoliposome stabilized by sea cucumber saponins instead of cholesterol. J Agric Food Chem 2020;68(2):642–51.
[17] Zhu Y, Liang J, Gao C, Wang A, Xia J, Hong C, et al. Multifunctional ginsenoside Rg3-based liposomes for glioma targeting therapy. J Controlled Release 2021;330:641–57.
[18] Hong C, Liang JM, Xia JX, Zhu Y, Guo YZ, Wang AN, et al. One stone four birds: A novel liposomal delivery system multi-functionalized with ginsenoside Rh2 for tumor targeting therapy. Nano-Micro Letters 2020;12(1):18.
[19] Qi LW, Wang CZ, Yuan CS. American ginseng: Potential structure-function relationship in cancer chemoprevention. Biochem Pharmacol 2010;80(7):947–54.
[20] Quan K, Liu Q, Wan JY, Zhao YJ, Guo RZ, Alolga RN, et al. Rapid preparation of rare ginsenosides by acid transformation and their structure-activity relationships against cancer cells. Sci Rep 2015;5(1):1–7.
[21] Dong H, Bai LP, Wong VKW, Zhou H, Wang JR, Liu Y, et al. The *in vitro* structure-related anti-cancer activity of ginsenosides and their derivatives. Molecules 2011;16(12):10619–30.
[22] Li W, Liu Y, Zhang JW, Ai CZ, Xiang N, Liu HX, et al. Anti-androgen-independent prostate cancer effects of ginsenoside metabolites *in vitro*: mechanism and possible structure-activity relationship investigation. Arch Pharmacal Res 2009;32(1):49–57.
[23] Lheureux G P, Fragata M. Micropolarities of lipid bilayers and micelles .5. localization of pyrene in small unilamellar phosphatidylcholine vesicles. Biophys Chem 1988;30(3):293–301.
[24] Kaiser RD, London E. Location of diphenylhexatriene (DPH) and its derivatives within membranes: comparison of different fluorescence quenching analyses of membrane depth. Biochemistry 1998;37(22):8180–90.
[25] Hu CM, Fang RH, Wang KC, Luk BT, Thamphiwatana S, Dehaini D, et al. Nanoparticle biointerfacing by platelet membrane cloaking. Nature 2015;526(7571):118–21.
[26] Thompson AMG, Iancu CV, Thi Thanh Hanh N, Kim D, Choe JY. Inhibition of human GLUT1 and GLUT5 by plant carbohydrate products; insights into transport specificity. Sci Rep 2015;5(1):1–10.
[27] Iancu CV, Zamoon J, Woo SB, Aleshin A, Choe JY. Crystal structure of a glucose/H^+ symporter and its mechanism of action. Proc Nat Acad Sci USA 2013;110(44):17862–7.
[28] Avril N. GLUT1 expression in tissue and 18F-FDG uptake. J Nucl Med 2004;45(6):930–2.
[29] Brown RS, Wahl RL. Overexpression of glut-1 glucose transporter in human breast cancer an immunohistochemical study. Cancer 1993;72(10):2979–85.
[30] Hussein YR, Bandyopadhyay S, Semaan A, Ahmed Q, Albashiti B, Jazaerly T, et al. Glut-1 expression correlates with basal-like breast cancer. Translational Oncology 2011;4(6):321–7.
[31] Cantuaria G, Fagotti A, Ferrandina G, Magalhaes A, Nadji M, Angioli R, et al. GLUT-1 expression in ovarian carcinoma: association with survival and response to chemotherapy. Cancer 2001;92(5):1144–50.
[32] Brown RS, Wahl RL. Overexpression of glut-1 glucose-transporter in human breast-cancer - an immunohistochemical study. Cancer 1993;72(10):2979–85.
[33] Krzeslak A, Wojcik-Krowiranda K, Forma E, Jozwiak P, Romanowicz H, Bienkiewicz A, et al. Expression of GLUT1 and GLUT3 glucose transporters in endometrial and breast cancers. Pathology Oncology Research 2012;18(3):721–8.